Salicylaldimine-Functionalized Poly(*m*-Phenyleneethynylene) as Turn-on Chemosensor for Ferric Ion

Nopparat Thavornsin,[1] Paitoon Rashatasakhon,[2] Mongkol Sukwattanasinitt,[2] Sumrit Wacharasindhu [2]

[1]Program of Petrochemistry and Polymer Science, Faculty of Science, Chulalongkorn University, Bangkok 10330, Thailand
[2]Department of Chemistry, Faculty of Science, Nanotec-CU Center of Excellence on Food and Agriculture, Chulalongkorn University, Bangkok 10330, Thailand
Correspondence to: S. Wacharasindhu (E-mail: sumrit.w@chula.ac.th)

Received 18 January 2018; accepted 27 February 2018; published online 24 March 2018
DOI: 10.1002/pola.28997

ABSTRACT: A new turn on fluorescent probe for ferric ion based on poly(*m*-phenyleneethynylene salicylaldimine) (**PPE-IM**) has been developed. The preparation of **PPE-IM** involves post-polymerization functionalization of the corresponding polymeric amine, **PPE-AM**, via the condensation with salicylaldehyde. The degree of polymerization of both **PPE-IM** and **PPE-IM** is 17 with polydispersity index of 1.5. In aqueous solution, the polymeric **PPE-IM** is highly stable unlike its small molecule analog which is gradually hydrolyzed. The weak fluorescence of initial **PPE-IM** ($\lambda_{em} = 470$) is greatly enhanced by 300 folds upon the addition of Fe^{3+}. The ^1H NMR reveals that the fluorescence enhancement is caused by Fe^{3+}-induced hydrolysis of the imine group. The sensing system shows a detection limit of 0.14 μM of Fe^{3+}. © 2018 Wiley Periodicals, Inc. J. Polym. Sci., Part A: Polym. Chem. **2018**, *56*, 1155–1161

KEYWORDS: chemodosensor; ferric ion; hydrolysis; poly(*m*-phenyleneethynylene salicylaldimine); Schiff base probe; turn on fluorescence

INTRODUCTION Application of conjugated polymer (CP)-based optical sensory materials in environmental monitoring and biomedical diagnostics has drawn great attention in recent year.[1–6] In comparison to small molecules, the CP-based sensor exhibit greater absorption cross section, extinction coefficient and thermal stability.[7–9] For fluorescent CP such as poly(phenyleneethynylene) (PPE), the lateral attachment of substituents on the aromatic ring with suitable receptor unit provides efficient sensor-based PPE.[10–14] The π–π^* conjugated electronic structure in PPE allows a fast excitation energy transfer along the backbone to the energy/electron acceptors which allows amplification of fluorescent signal.[15–18] With this property, numerous of highly sensitive PPEs sensor was designed and reported as fluorescence quenching (turn-off) mode via single quencher molecule (analyte) causing an efficient quenching of the long polymer segment.[19–22] In principle, fluorescence "turn-on" sensor has numerous advantages over "turn-off" sensors, for example: (1) higher sensitivity as a result of contrasting fluorescence signal with a dark background (2) higher selectivity as the signal is generated by specific binding, whereas fluorescence quenching can occur in multiple ways. Despite these advantages, designing a highly selective and sensitive fluorescence turn on sensor from conjugated polymer is challenging since a strong emissive background from initial highly conjugated backbone of polymer must be suppressed. To date, a few PPEs turn-on sensors were reported for metal sensing. These are based on the inhibition of aggregation,[23,24] photo-induced electron transfer (PET),[25,26] and intramolecular charge transfer (ICT)[27] mechanisms. It is still desirable to enhance the specificity and sensitivity of this class of PPE-based turn on sensor for important metal ion.

Iron is a crucial element in the biological systems. Elevated level of Fe^{3+} ion within the body has been associated with increased incidence of cancer as well as dysfunction of critical organs such as the heart, pancreas, and liver.[28,29] Thus, monitoring and detection of Fe^{3+} is important. Previously, most fluorescent probes for Fe^{3+} ion were reported as turn off mode based on the paramagnetic nature of Fe^{3+}.[30,31] However, in recent years, fluorescent turn-on probes for Fe^{3+} based on small molecules were emerging as a new sensor design concept. Generally, salicylaldimine Schiff base is incorporated as a receptor into the chromophores.[32–37] Owing to isomerization of C═N and ESIPT from salicylaldimine group, those probes show weak fluorescent signals in the initial state. The addition of

Additional Supporting Information may be found in the online version of this article.

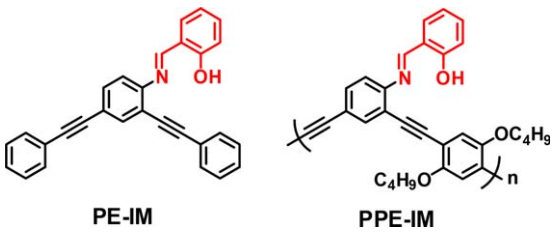

FIGURE 1 Structure of **PE-IM** and **PPE-IM**. [Color figure can be viewed at wileyonlinelibrary.com]

Fe^{3+} ion promotes the hydrolysis of salicylaldimine group and return into the high emissive chromophores. This strategy creates the Fe^{3+} chemodosensor as fluorescence turn-on probe in which the fluorescence signal is not only irreversible but the probes also act as scavenges of Fe^{3+} in the physiological environment. However, the only drawback of this strategy is that the hydrolysis of salicylaldimine group may prematurely undergo in aqueous media causing not only the instability of probes itself but also false turn-on fluorescence signal.

In this study, we prepared a highly stable and selective fluorescence turn on probe for Fe^{3+} detection based on poly(-phenyleneethynylene) containing salicylaldimine **PPE-IM** peripheral group (Fig. 1). The salicylaldimine groups have dual roles as a Fe^{3+} receptor and fluorescence quencher. The probe has a sufficiently dark fluorescence background which is a prerequisite for turn-on sensing probe. The polymeric structure facilitates both aggregation and self-coiling to protect the imine group from hydrolysis. This behavior results in a highly stable probe in aqueous media. For comparison purpose, we construct a small molecule analog, **PE-IM**, to be studied alongside **PPE-IM**.

EXPERIMENTAL

Materials

All reactions were carried out under nitrogen atmosphere using freshly anhydrous solvents. All reagents were purchased from Sigma-Aldrich (USA), Fluka® (Switzerland), TCI chemical (Japan), or Merck® (Germany) and used without further purification.

Measurements

Analytical thin-layer chromatography (TLC) was performed on Kieselgel F-254 pre-coated plastic TLC plates from EM Science. Visualization was performed with a 254 nm ultraviolet lamp. Gel column chromatography was carried out with silica gel 60 (70–230 mesh) from Merck. Elemental (C, H, N) analysis was performed on PE 2400 series II (Perkin-Elmer, USA). The ^1H and ^{13}C NMR spectra were recorded on a Varian 400 or Bruker 400 in $CDCl_3$, THF-d_8 or $(CD_3)_2CO$. Chemical shifts are expressed in parts per million (δ) using residual solvent protons as internal standards: $CDCl_3$ (δ 7.26 for ^1H, δ 77.00 for ^{13}C), THF-d_8 (δ 1.72, 3.58 for ^1H) and $(CD_3)_2CO$ (δ 2.05 for ^1H, δ 206.26 for ^{13}C). Fourier transform infrared spectra were acquired on Nicolet 6700 FTIR spectrometer equipped with a mercury-cadmium telluride (MCT) detector (Nicolet, USA). All polymer solutions were filtered through 0.45 μm syringe filters prior to use. Polymer molecular weights were determined by Waters 600 controller chromatograph equipped with two HR (waters), column (HR1 and HR4) at 35 °C and a reflective index detector (waters 2414). Tetrahydrofuran (HPLC grade) was used as the eluent with the flow rate of 1.0 mL/min (4 mg/mL sample concentrations). Sample injection volume was 50 μL. Polystyrenes (996–188,000 Da) were used as standards for calibration. The UV–visible spectra were

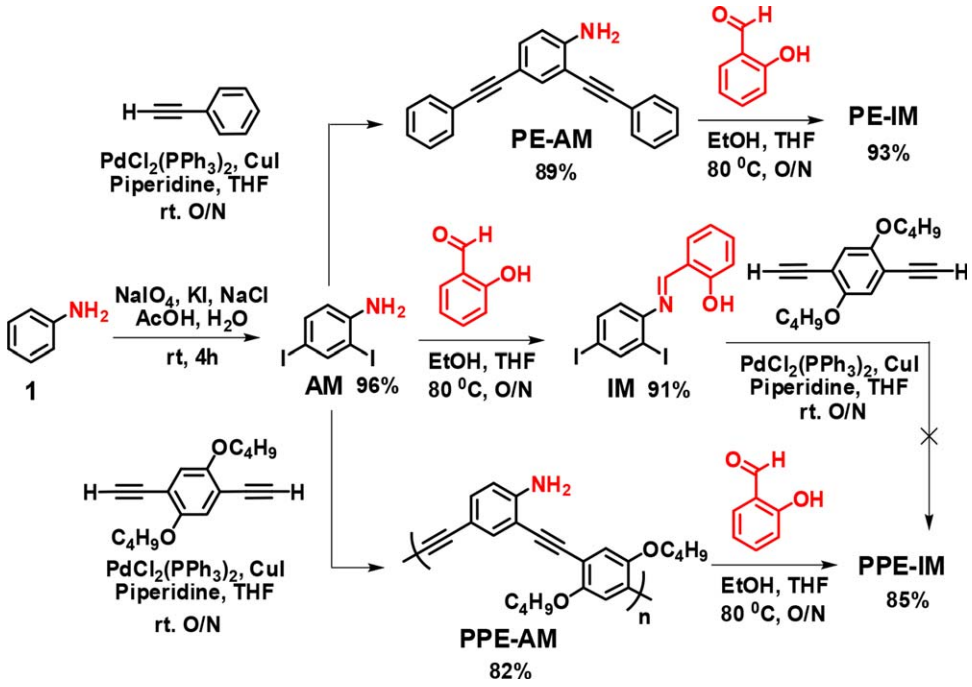

SCHEME 1 Synthesis routes of **PE-IM** and **PPE-IM**. [Color figure can be viewed at wileyonlinelibrary.com]

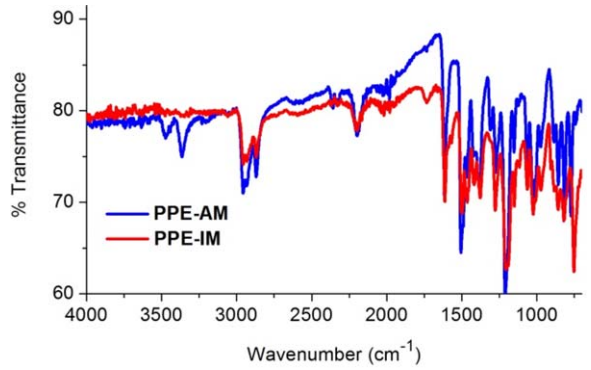

FIGURE 2 FTIR spectra of **PPE-AM** and **PPE-IM**. [Color figure can be viewed at wileyonlinelibrary.com]

obtained from Varian Cary 50 UV–Vis spectrophotometer (Varian, USA) and the fluorescence emission spectra were recorded on a Varian Cary Eclipse spectrofluorometer (Varian, USA) using a quartz cuvette with 1 cm beam path length at room temperature with excitation and emission slit widths of 10 nm and 10 nm, respectively.

Synthesis of 2,4-Diiodoaniline (AM)

This compound was prepared according to a previous literature report.[20] ^{1}H NMR (400 MHz, ($CDCl_3$) δ 7.89 (s, 1H), 7.37 (d, $J = 8.4$ Hz, 1H), 6.52 (d, $J = 8.4$ Hz, 1H), 4.13 (s, 2H).

Synthesis of (*E*)-2-((2,4-Diiodophenylimino) Methyl)Phenol (IM)

A mixture of **AM** (100 mg, 0.29 mmol), salicylaldehyde (33.87 μL, 0.32 mmol) in EtOH (3 mL) was stirred at 80 °C for 3 h. The precipitated bright yellow solid was washed with cold EtOH (3 × 25 mL) to obtain desired product (yield: 118.2 mg, 91%) ^{1}H NMR (400 MHz, $(CD_3)_2CO$) δ 12.69 (s, 1H), 8.86 (s, 1H), 8.33 (s, 1H), 7.87 (d, $J = 7.4$ Hz, 1H), 7.63 (m, 1H), 7.48 (m, 1H), 7.31 (d, $J = 7.0$ Hz, 1H), 7.00 (d, $J = 7.7$ Hz, 2H). ^{13}C NMR (101 MHz, $(CD_3)_2CO$) δ 166.08, 162.15, 147.57, 139.91, 134.99, 134.37, 121.65, 120.37, 120.17, 120.13, 118.05, 117.95, 98.40, 92.25. MALDI-TOF MS calcd. $C_{13}H_9I_2NO$ 448.877, found 450.042.

Synthesis of 2,4-Bis(Phenylethynyl)Aniline (PE-AM)

A typical procedure was followed according to the literature.[38] A yellow powder of **PE-AM** was obtained. ^{1}H NMR (400 MHz, $(CD_3)_2CO$) δ 7.62–7.57 (m, 2H), 7.49 (d, $J = 8.2$ Hz, 3H), 7.43–7.33 (m, 6H), 7.28 (d, $J = 8.5$ Hz, 1H), 6.83 (d, $J = 8.5$ Hz, 1H), 5.57 (s, 2H). FTIR (neat, cm^{-1}) 3465, 3373, 3029, 2362, 2202, 1612, 1500. MALDI-TOF MS calcd. $C_{22}H_{15}N$ 293.1204, found 292.2350.

Synthesis of (*E*)-2-((2,4-Bis(Phenylethynyl) Phenylimino)Methyl)Phenol (PE-IM)

Compound **PE-AM** (94 mg, 0.32 mmol) was dissolved in 2.5 mL of EtOH and the solution was stirred at 50 °C for 15 min after the addition of salicylaldehyde (40.8 μL, 0.38 mmol). The reaction mixture was stirred at reflux for 2 h. After filtration, the filter was collected and washed with cold EtOH (5 × 10 mL). After drying under vacuum, an orange powder (**PE-IM**) was obtained (yield: 118 mg, 93%) ^{1}H NMR (400 MHz, $(CD_3)_2CO$) δ 13.51 (s, 1H), 9.12 (s, 2H), 7.83 (s, 2H), 7.68 (dd, $J = 8.0$, 2.1 Hz, 10H), 7.62–7.58 (m, 4H), 7.50–7.43 (m, 14H), 7.00 (dd, $J = 14.2$, 7.6 Hz, 4H). ^{13}C NMR (101 MHz, $(CD_3)_2CO$) δ 165.10, 165.06, 162.56, 162.16, 149.83, 136.33, 134.68, 134.08, 133.45, 132.65, 132.42, 129.71, 129.65, 129.52, 129.44, 123.81, 123.77, 122.84, 120.78, 120.33, 120.10, 120.03, 119.27, 118.00, 117.90, 96.03, 91.45, 88.90, 86.67. FTIR (neat, cm^{-1}) 3055, 2359, 2201, 1606. MALDI-TOF MS calcd. $C_{29}H_{19}NO$ 397.1467, found 397.4780.

Synthesis of PPE-AM

In a typical experiment, a mixture of compound **AM** (100 mg, 0.29 mmol), 1,4-dibutoxy-2,5-diethynylbenzene[39] (78.4 mg, 0.29 mmol), $PdCl_2(PPh_3)_2$ (20.4 mg, 0.03 mmol), CuI (11.0 mg, 0.06 mmol), PPh_3 (15.2 mg, 0.06 mmol) were stirred in the mixture solvent of THF (2 mL) and DBU (1 mL). The reaction was carried out under pressure of N_2 filled in rubber balloons and stirred at room temperature for 24 h. Then the solution was added with dichloromethane (10 mL) to dissolve part of the jelly polymer for 15 min. The solution was concentrated under reduced pressure to a small volume (≈1 mL) and the polymer was precipitated by dropping the concentrated solution into 150 mL of cold methanol. The precipitate that formed was collected by centrifuge, washed repeatedly with methanol (5 × 30 mL) and evaporated under vacuum to afford greenish yellow powder of **PPE-AM** (yield: 85 mg, 82%) $M_w = 6.3 \times 10^3$ Da, DP = 17, PDI = 1.5, ^{1}H NMR (400 MHz, $CDCl_3$) δ 7.86, 7.57, 7.29, 7.00, 6.71, 4.76, 4.05, 1.85, 1.58, 1.03. ^{13}C NMR (101 MHz, $CDCl_3$) δ 155.08, 153.29, 148.29, 142.02, 134.52, 133.12, 132.65, 117.90, 116.94, 116.72, 116.41, 115.78, 115.16, 113.86, 107.93, 92.19, 84.92, 84.15, 82.84, 69.47, 68.92, 31.44, 19.22, 13.90. FTIR (neat, cm^{-1}) 3470, 3362, 2958, 2866, 2357, 2190, 1612, 1506, 1211.

Synthesis of PPE-IM

Polymer **PPE-AM** (67 mg, 0.18 mmol based on repeating unit) was dissolved in 2 mL of EtOH at 70 °C for 15 min. Then salicylaldehyde (540 mg, 0.47 mL) was added and the reaction was stirred for 24 h. The reaction mixture was cooled to room temperature and concentrated to small volume by rotary evaporator before precipitation in cold

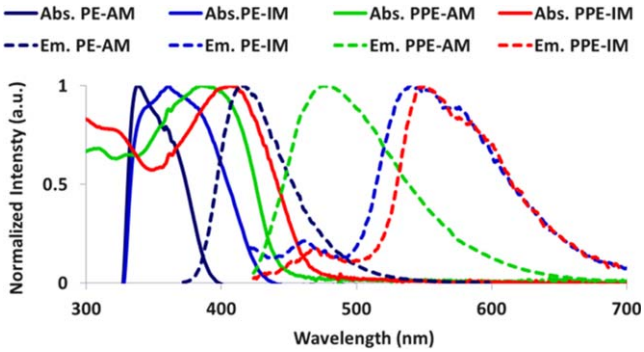

FIGURE 3 Normalized spectra of absorption and emission of **PE-AM**, **PE-IM**, **PPE-AM**, and **PPE-IM**. [Color figure can be viewed at wileyonlinelibrary.com]

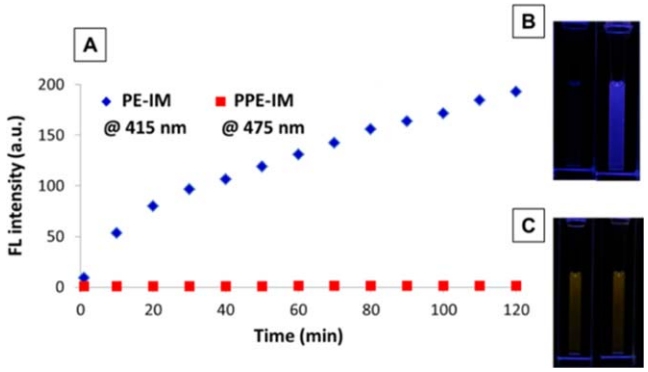

FIGURE 4 (A) Time dependence of fluorescence intensity, at λ_{em}, of **PE-IM** (25 μM) and **PPE-IM** (25 μM) in 10% MilliQ water/THF ($\lambda_{ex} = 340$ nm). Photographic images under black-light of (B) **PE-IM** and (C) **PPE-IM** at 0 and 120 min, respectively. [Color figure can be viewed at wileyonlinelibrary.com]

methanol. After precipitated polymer was formed, there was collected by centrifuge and washed repeatedly with cold methanol (5 × 30 mL) to afford orange powder of **PPE-IM** (yield: 75 mg, 85%). ^{1}H NMR (400 MHz, ($CDCl_3$) δ 13.44, 12.83, 8.79, 8.57, 8.12, 7.77, 7.54, 7.43, 7.29, 6.98, 4.05, 1.83, 1.55, 1.02. ^{13}C NMR (101 MHz, $CDCl_3$) δ 162.63, 161.49, 153.67, 153.32, 149.13, 148.59, 142.04, 136.79, 135.55, 133.41, 132.58, 132.43, 132.33, 119.15, 118.94, 117.38, 117.14, 96.05, 92.04, 91.22, 69.35, 68.88, 31.15, 19.11, 13.75, FTIR (neat, cm^{-1}) 2955, 2929, 2866, 2193, 1609, 1497, 1205.

UV–Vis and Fluorescence Analysis

The stock solutions of all polymers (**PPE-AM, PPE-IM**) in THF and small molecules (**PE-AM**, **PE-IM**) in acetone were prepared at a concentration of 1.0 × 10^{-3} M and diluted with a THF-MilliQ mixture (9/1, v/v) as required before use. The absorption spectra of all compounds were determined from 250 nm to 600 nm. The emission spectra were recorded from 350 nm to 700 nm using an excitation wavelength at 300 to 410 nm at ambient temperature. The metal ion stock solutions were prepared by dissolving the metal salts in deionized water at a concentration of 10.0 × 10^{-3} M and were diluted as required before use. A solution of the test sample (1.0 mL, 10 μM for fluorescence and UV–vis) was placed in a quartz cell (10.0 mm width), and the UV–vis and fluorescence spectra were recorded respectively by measuring the changes of intensity after mixing for 60 min.

RESULTS AND DISCUSSION

Synthesis of Imine Derivatives (PE-IM and PPE-IM)

The synthetic routes of **PE-IM** and **PPE-IM** are depicted in Scheme 1. The model compound **PE-IM** was prepared in high yield from diiodoaniline (**AM**) via two straightforward steps. The Sonogashira coupling reaction between **AM** with phenylacetylene gave **PE-AM** followed by the condensation with salicylaldehyde to yield the desired **PE-IM**. For the synthesis of **PPE-IM**, our initial attempt to condense AM with salicylaldehyde led to a hydrolytically unstable imine, **IM**.[40] Moreover, an attempt to polymerize **IM** into **PPE-IM** gave polymeric material with only low degree of polymerization. This is probably due to strong chelation of salicylaldimine to Pd species.[41,42] Fortunately, **PPE-IM** could be obtained via post-polymerization functionalization (PPF) of **PPE-AM** via the condensation with salicylaldehyde. Conversion of **PPE-AM** into **PPE-IM** is clearly observed by FTIR (Fig. 2). The N—H stretching of amine group in **PPE-AM** at 3470 and 3365 cm^{-1} disappeared. Further confirmation was provided by ^{1}H NMR spectra which showed complete disappearance of the amine protons (—NH_2), at 4.76 ppm, and the aromatic proton vicinal to the amine, at 6.98 ppm, that indicated an efficient PPF [Supporting Information Fig. S1(A)]. Moreover, the aromatic proton from both salicylaldehyde ($\delta = 8.12$–8.57 ppm) and aniline ($\delta = 8.79$ ppm) was also observed. Interestingly, two high chemical shifts at 12.83 and 13.44 ppm corresponding to the intramolecular hydrogen bonded phenolic protons of **PPE-IM** in the possible head–head and head–tail orientation [Supporting Information Fig. S1(B)]. The disappearance of both peaks upon addition of CD_3OD confirms that both peaks are exchangeable protons.[43] We also would like to note that unlike **IM** or **PE-IM** that gradually undergoes hydrolysis upon storage in $CDCl_3$, **PPE-IM** is stable for more than a week without detectable hydrolysis products. From GPC measurement, the molecular weight (M_w) of **PPE-IM** was 8455 Da corresponding to ~100% condensation of salicylaldehyde on **PPE-AM** ($M_w = 6253$ Da) (Supporting Information Figs. S2 and S3). To the best of our knowledge, this is the first report on post-polymerization functionalization of PPE via imination that the methodology is very effective and convenient.

The UV–vis absorption and fluorescence emission spectra of fluorophore **PE-AM**, **PE-IM**, **PPE-AM**, and **PPE-IM** are shown in Figure 3 and the photophysical properties are summarized in Table S1. In comparison with the small molecule model (**PE-AM**), the polymeric **PPE-AM** exhibited a significantly longer absorption and emission wavelength that can be

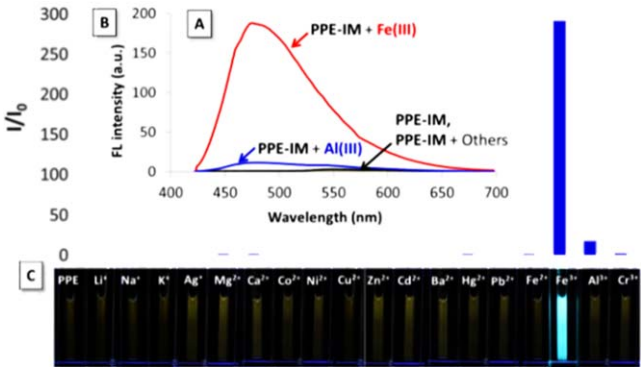

FIGURE 5 (A) Fluorescent spectra ($\lambda_{ex} = 410$ nm) of **PPE-IM** (25 μM) upon the addition of various metal ions (5 equiv.) in 10% MilliQ water/THF, (B) corresponding fluorescence intensity ratio (I/I_0) at $\lambda_{em} = 476$ nm and (C) photographic images of corresponding solution of **PPE-IM** in the presence of different cations. All data were recorded after 30 min of mixing. [Color figure can be viewed at wileyonlinelibrary.com]

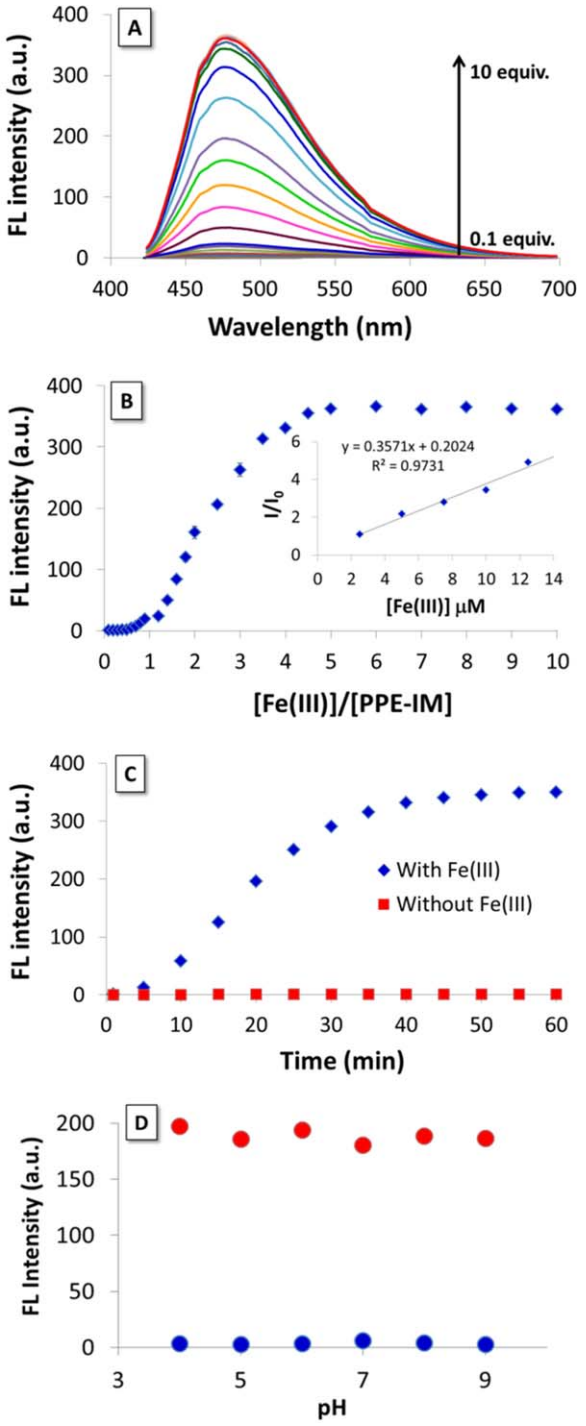

FIGURE 6 (A) and (B) Fluorescence titration ($\lambda_{ex} = 410$ nm) of **PPE-IM** (25 μM) with Fe^{3+} in 10% MilliQ water/THF. The inset shows the calibration curves of ratio of **PPE-IM** to Fe^{3+} concentration. Each spectrum was obtained after 60 min of mixing. (C) Time dependence of fluorescence intensity of **PPE-IM** (25 μM) in the presence and absence of Fe^{3+} (5 equiv.) at pH 3.5. (D) FL intensity of **PPE-IM** (25 μM) before (blue dots) and after (red dots) addition of $Fe(NO_3)_3$ (125 μM) after 30 min of mixing at various pH. [Color figure can be viewed at wileyonlinelibrary.com]

attributed to the longer π conjugation system in our polymer backbone. The imination of **PE-AM** to **PE-IM** and **PPE-AM** to **PPE-IM** resulted in two emission bands (469 and 545). The first band at 469 nm in **PE-IM** and **PPE-IM** corresponds to the relaxation of the normal phenol tautomer while the second band at 545 nm corresponds to the relaxation of the keto tautomer formed by the excited induced proton transfer process (ESIPT). The ESIPT is usually accompanied by a large stroke shift values as large as 140–180 nm.[44] The formation of salicylaldimine Schiff base also significantly suppresses fluorescent quantum yields of **PE-IM** and **PPE-IM** ($\Phi_f \ll 0.01$) in comparison with the corresponding amines ($\Phi_f > 0.20$). The low fluorescent quantum yields are attributed to the combination of ESIPT and C=N isomerization processes. Importantly, these results confirm the success of our structural design in using salicylaldimine to suppress the initial fluorescence signal of the turn-on fluorescent sensor.

Stability Test

For the stability test, fluorescence of **PPE-IM** and **PE-IM** were monitored in 10% MilliQ water/THF for 2 h [Fig. 4(A)]. The fluorescence intensity at 415 nm of **PE-IM** increased along with bright blue appearance [Fig. 4(B)]. This result suggested that the imine was hydrolyzed back to **PE-AM** confirmed by matching of the emission spectrum with the original **PE-AM** [Supporting Information Fig. S4(A)]. However, no fluorescence change of **PPE-IM** under the same condition and its appearance remained dark under black-light [Fig. 4(C)]. Moreover, the fluorescence of **PPE-IM** is stable under broad pH range of 4–8 (Supporting Information Fig. S5). This result supports our hypothesis that salicylaldimine Schiff base could be stabilized by incorporating into the polymer chain.

Metal Cation Detection

The sensing ability of **PPE-IM** was screened with various metal ions investigated in 10% MilliQ water/THF. The absorption spectra of **PPE-IM** changed only slightly with the addition of each metal ion (Supporting Information Fig. S6). In fluorescence measurement, however, the addition of Fe^{3+} (125 μM) caused

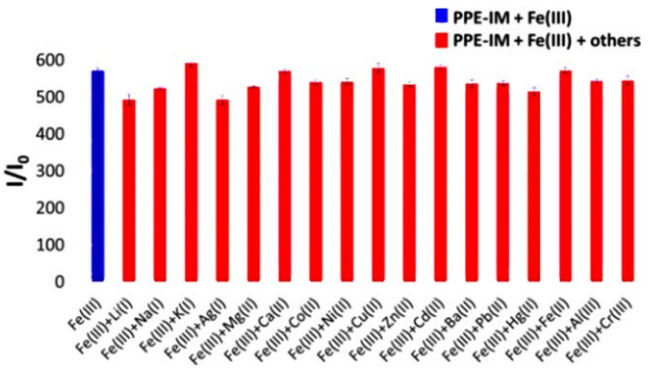

FIGURE 7 Relative fluorescence of **PPE-IM** (25 μM) in 10% MilliQ water/THF in the presence of Fe^{3+} (125 μM) plus another metal ion (625 μM) tested for interference. Each spectrum was obtained after 60 min of mixing. [Color figure can be viewed at wileyonlinelibrary.com]

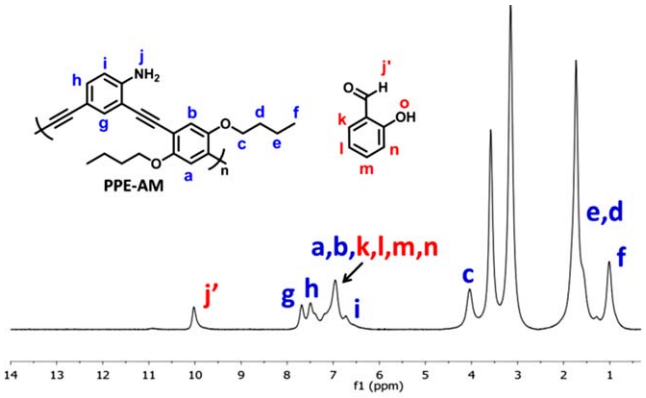

FIGURE 8 ^{1}H NMR of **PPE-IM** in THF-d_8 after addition of $Fe(NO_3)_3$ (10 equiv.) at 30 min. [Color figure can be viewed at wileyonlinelibrary.com]

a marked increase in fluorescence intensity at 476 nm by over 300-fold after 30 min (Fig. 5). The increase in water contents in the system resulted in lower fluorescent sensing ability (Supporting Information Fig. S7). This may be caused by the water induced aggregation-caused quenching (ACQ)[45,46] of both **PPE-AM** and **PPE-IM**. Notably, the addition of Fe^{3+} to **PPE-AM** gave insignificant fluorescent change under the same condition (Supporting Information Fig. S8). This result suggested the hydrolysis of imine moiety of **PPE-IM** responds for increase in fluorescent signal upon the addition of Fe^{3+}. Also, the **PPE-IM**/Fe^{3+} mixed solution showed bright blue luminescence which remained unchanged for several hours [Fig. 5(C)]. For other metal ions such as Li^+, Na^+, K^+, Ag^+, Mg^{2+}, Ca^{2+}, Co^{2+}, Ni^{2+}, Cu^{2+}, Zn^{2+}, Cd^{2+}, Ba^{2+}, Hg^{2+}, Pb^{2+}, Fe^{2+}, Al^{3+}, and Cr^{3+}, the fluorescence intensity of **PPE-IM** remained relatively unchanged except slight increase with Al^{3+}. Therefore, **PPE-IM** could serve as a stable and selective turn-on fluorescent probe for Fe^{3+} sensing.

The time-dependence investigation showed that the fluorescence signal increased and became saturated after 60 min after the addition of 250 μM Fe^{3+} (Supporting Information Fig. S9). The measurements of fluorescence intensity of all subsequence experiments were thus performed after 60 min of mixing to ensure the completion of the reaction and signal stability. The fluorescence quantum efficiency (Φ_f) was increased from <0.01 to 0.38. For quantitative analysis, the titration of Fe^{3+} at variable concentration was performed and the fluorescence emission was measured at 60 min to ensure the signal saturation [Fig. 6(A)]. A good linear fluorescence response was obtained in the Fe^{3+} concentration range of 2–12 μM [Fig. 6(B)]. The detection limit at threefold standard deviation ($3\sigma/K$ whereas σ = standard deviation of the fluorescence intensity of the **PPE-IM** solution in the absence of Fe^{3+}; and K = slope of the calibration line)[47] was 0.14 μM [Fig. 6(B inset)]. We would like to emphasize that the acidity of $Fe(NO)_3$ in aqueous solution is not responsible for the hydrolysis of imine which is a probable cause of the fluorescence enhancement. In control experiment at the same pH of 3.5 but without Fe^{3+}, the fluorescence intensity was insignificantly changed. This result strongly supports that the fluorescence enhancement of **PPE-IM** is caused by Fe^{3+} [Fig. 6(C)] induced hydrolysis. We also examined pH-tolerance limit in **PPE-IM** sensing ability in the pH range between 4 and 9. The fluorescent enhancement remained the same as shown in Figure 6(D).

To evaluate the interference from other metal ions, competition experiments were carried out by addition of Fe^{3+} and another metal cation (5 equiv. of Fe^{3+}) tested for interference to the **PPE-IM** solution (Fig. 7). In the presence of other competing metal cations including Li^+, Na^+, K^+, Ag^+, Mg^{2+}, Ca^{2+}, Co^{2+}, Ni^{2+}, Cu^{2+}, Zn^{2+}, Cd^{2+}, Ba^{2+}, Pb^{2+}, Hg^{2+}, Fe^{2+}, Al^{3+}, and Cr^{3+}, no significant interference was observed. The results indicate that **PPE-IM** is very selective for Fe^{3+} detection and quantification.

To gain more mechanistic information of this turn-on phenomenon, the ^{1}H NMR were used to monitor the titration between $Fe(NO_3)_3$ with **PPE-IM** in THF-d_8 (Fig. 8). Upon the addition of 10 equiv. $Fe(NO_3)_3$, imine proton signal (*j*) at 9.01 ppm disappeared along with the increase in peak at 10.02 ppm (*j'*) corresponding to the proton of aldehyde group of salicylaldehyde. Furthermore, the proton signal of aromatic region at 6.71 ppm (*i*) emerged, which is match with *otho*-position of aniline proton in original **PPE-AM**. In its absorption spectra, the new broaden band at 380 nm is increased which can be assigned to the salicylaldehyde residue (Supporting Information Fig. S10). These evidences indicated that irreversible binding of Fe^{3+} ion with **PPE-IM** induced the reformation of **PPE-AM**. This is caused by the cleavage of imine by Fe^{3+}-catalyzed hydrolysis process.

To investigate the effect of intramolecular hydrogen bonding interaction on conformation change of our polymer, we further measured the particle size of **PPE-IM** before and after treatment with $Fe(NO_3)_3$ solution. The increase in particle size was observed upon addition of Fe^{3+} to the polymer solution (Supporting Information Fig. S11). The result suggested that the addition of Fe^{3+} not only resulted in the hydrolysis of **PPE-IM** to **PPE-AM** but also caused some aggregation[48] of the resulting **PPE-AM** (Fig. 9).

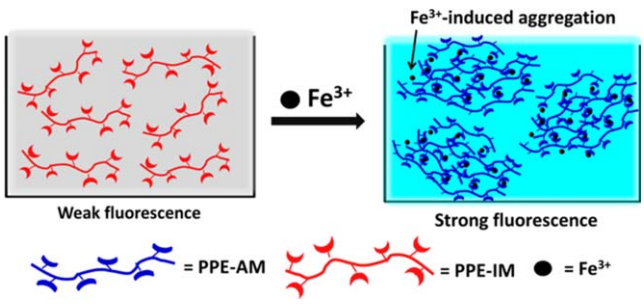

FIGURE 9 Schematic representation of the plausible behavior of the **PPE-IM** before and after treatment with Fe^{3+}. [Color figure can be viewed at wileyonlinelibrary.com]

CONCLUSIONS

In conclusion, a new conjugated polymeric sensor based on salicylaldimine-functionalized poly(*m*-phenyleneethynylene)s was successfully synthesized in excellent yield via Sonogashira coupling reaction and post-polymerization functionalization. A well define Schiff base polymer provides high hydrolytic stability in a wide pH range. This is caused by strong intramolecular hydrogen bonding and hydrophobic interaction among the side chains. The probe displays remarkably sensitive and selective fluorescence turn-on towards Fe^{3+}, through metal-promoted hydrolysis process, with low detection limit of 0.14 μM and without significant interference from other metal ions. Thus, **PPE-IM** developed herein could be a promising material for Fe^{3+} selective detection. It can be useful in several biological and environmental analysis as well as early rust detection.

ACKNOWLEDGMENTS

This study is financially supported by the Thailand Research Fund (TRF-RSA6080018) and Nanotechnology Center (NANOTEC), NSTDA, Ministry of Science and Technology, Thailand, through its International Research Integration: Chula Research Scholar, program of Center of Excellence Network, Ratchadapiseksomphot Endowment Fund of Chulalongkorn University, Center of Excellence on Petrochemicals and Materials Technology (PETROMAT).

REFERENCES AND NOTES

1 H. Jiang, P. Taranekar, J. R. Reynolds, K. S. Schanze, *Angew. Chem. Int. Ed.* **2009**, *48*, 4300.

2 C. Gu, N. Huang, J. Gao, F. Xu, Y. Xu, D. Jiang, *Angew. Chem. Int. Ed.* **2014**, *53*, 4850.

3 J. X. Jiang, F. Su, A. Trewin, C. D. Wood, N. L. Campbell, H. Niu, C. Dickinson, A. Y. Ganin, M. J. Rosseinsky, Y. Z. Khimyak, A. I. Cooper, *Angew. Chem. Int. Ed.* **2007**, *46*, 8574.

4 C. Zhu, L. Liu, Q. Yang, F. Lv, S. Wang, *Chem. Rev.* **2012**, *112*, 4687.

5 F. J. M. Hoeben, P. Jonkheijm, E. W. Meijer, A. P. H. J. Schenning, *Chem. Rev.* **2005**, *105*, 1491.

6 D. T. McQuade, A. E. Pullen, T. M. Swager, *Chem. Rev.* **2000**, *100*, 2537.

7 Y.-J. Cheng, S.-H. Yang, C.-S. Hsu, *Chem. Rev.* **2009**, *109*, 5868.

8 A. P. H. J. Schenning, E. W. Meijer, *Chem. Commun.* **2005**, *26*, 3245.

9 H. Zhou, L. Yang, W. You, *Macromolecules* **2012**, *45*, 607.

10 U. H. F. Bunz, *Macromol. Rapid Commun.* **2009**, *30*, 772.

11 T. Yamamoto, I. Yamaguchi, T. Yasuda, In *Poly(Aryleneethynylene)s: From Synthesis to Application*; C. Weder, Ed.; Springer, Berlin Heidelberg: Berlin, **2005**; pp 181–208.

12 R. R. Nambiar, G. L. Brizius, D. M. Collard, *Adv. Mater.* **2007**, *19*, 1234.

13 M. Ortiz, C. Yu, Y. Jin, W. Zhan, *Top. Curr. Chem.* **2017**, *375*, 69.

14 N. Thavornsin, M. Sukwattanasinitt, S. Wacharasindhu, *Polym. Chem.* **2014**, *5*, 48.

15 S. W. Thomas, G. D. Joly, T. M. Swager, *Chem. Rev.* **2007**, *107*, 1339.

16 L.-J. Fan, Y. Zhang, C. B. Murphy, S. E. Angell, M. F. L. Parker, B. R. Flynn, W. E. Jones, *Coord. Chem. Rev.* **2009**, *253*, 410.

17 S. Rochat, T. M. Swager, *ACS Appl. Mater. Interfaces* **2013**, *5*, 4488.

18 B. C. Popere, A. M. Della Pelle, A. Poe, G. Balaji, S. Thayumanavan, *Chem. Sci.* **2012**, *3*, 3093.

19 J. Han, M. Bender, K. Seehafer, U. H. F. Bunz, *Angew. Chem. Int. Ed.* **2016**, *55*, 7689.

20 X. Yong, W. Wan, M. Su, W. You, X. Lu, Y. Yan, J. Qu, R. Liu, T. Masuda, *Polym. Chem.* **2013**, *4*, 4126.

21 U. H. F. Bunz, K. Seehafer, M. Bender, M. Porz, *Chem. Soc. Rev.* **2015**, *44*, 4322.

22 B. Wang, J. Han, M. Bender, K. Seehafer, U. H. F. Bunz, *Macromolecules* **2017**, *50*, 4126.

23 H. Wang, F. He, R. Yan, X. Wang, X. Zhu, L. Li, *ACS Appl. Mater. Interfaces* **2013**, *5*, 8254.

24 X. Ji, Y. Yao, J. Li, X. Yan, F. Huang, *J. Am. Chem. Soc.* **2013**, *135*, 74.

25 L.-J. Fan, Y. Zhang, W. E. Jones, *Macromolecules* **2005**, *38*, 2844.

26 H. Xu, W. Wu, Y. Chen, T. Qiu, L. J. Fan, *ACS Appl. Mater. Interfaces* **2014**, *6*, 5041.

27 Y. Pourghaz, P. Dongare, D. W. Thompson, Y. Zhao, *Chem. Commun. (Camb.)* **2011**, *47*, 11014.

28 R. G. Stevens, D. Y. Jones, M. S. Micozzi, P. R. Taylor, *N. Engl. J. Med.* **1988**, *319*, 1047.

29 M. Tenenbein, *Arch. Pediatr. Adolesc. Med.* **2005**, *159*, 557.

30 N. Walker, *J. Chem. Educ.* **1977**, *54*, 431.

31 Y. Lei, H. Li, X. Huang, J. Chen, M. Liu, W. Gao, J. Ding, D. Lin, H. Wu, *Tetrahedron* **2015**, *71*, 3453.

32 W. Lin, L. Yuan, X. Cao, *Tetrahedron Lett.* **2008**, *49*, 6585.

33 W. Lin, L. Yuan, J. Feng, X. Cao, *Eur. J. Org. Chem.* **2008**, *2008*, 2689.

34 M. H. Lee, T. V. Giap, S. H. Kim, Y. H. Lee, C. Kang, J. S. Kim, *Chem. Commun.* **2010**, *46*, 1407.

35 Y.-Z. Chen, Y. R. Bhorge, A. J. Pape, R. D. Divate, Y.-C. Chung, Y.-P. Yen, *J. Fluoresc.* **2015**, *25*, 1331.

36 S. Samanta, S. Goswami, A. Ramesh, G. Das, *J. Photochem. Photobiol. A: Chem.* **2015**, *310*, 45.

37 B.-X. Shen, Y. Qian, *J. Mater. Chem. B* **2016**, *4*, 7549.

38 W. Zhang, P. C. Huang, *Mater. Chem. Phys.* **2006**, *96*, 283.

39 A. Harriman, L. J. Mallon, K. J. Elliot, A. Haefele, G. Ulrich, R. Ziessel, *J. Am. Chem. Soc.* **2009**, *131*, 13375.

40 W. Y. Kim, H. Shi, H. S. Jung, D. Cho, P. Verwilst, J. Y. Lee, J. S. Kim, *Chem. Commun.* **2016**, *52*, 8675.

41 T. Stringer, P. Chellan, B. Therrien, N. Shunmoogam-Gounden, D. T. Hendricks, G. S. Smith, *Polyhedron* **2009**, *28*, 2839.

42 M. Keleş, H. Keleş, D. M. Emir, *Appl. Organomet. Chem.* **2015**, *29*, 543.

43 M. A. Wendt, J. Meiler, F. Weinhold, T. C. Farrar, *Mol. Phys.* **1998**, *93*, 145.

44 T. Mutai, H. Sawatani, T. Shida, H. Shono, K. Araki, *J. Org. Chem.* **2013**, *78*, 2482.

45 G. v. Bünau, *Ber. Bunsenges. Phys. Chem.* **1970**, *74*, 1294.

46 X. Ma, R. Sun, J. Cheng, J. Liu, F. Gou, H. Xiang, X. Zhou, *J. Chem. Educ.* **2016**, *93*, 345.

47 K. Tiwari, M. Mishra, V. P. Singh, *RSC Adv.* **2013**, *3*, 12124.

48 J. Yang, D. Wu, D. Xie, F. Feng, K. S. Schanze, *J. Phys. Chem. B* **2013**, *117*, 16314.